Int. J. Electrochem. Sci., 16 **(2021)** Article ID: 21086, doi: 10.20964/2021.08.29

International Journal of
ELECTROCHEMICAL
SCIENCE
www.electrochemsci.org

Nanosized NiO Thin Films Fabricated by Sol-gel Method for Amperometric Detection of Hydrogen Peroxide at a Very Low Overpotential

Zeineb Kouki[1], *Abdelhak Othmani*[1,*], *Mouldi Zouaoui*[1], *Adel Madani*[1,2]

[1] Université de Carthage, Faculté des Sciences de Bizerte, LR01 ES15, Laboratoire de Physique des Matériaux : Structure et Propriétés, 7021 Zarzouna, Bizerte, Tunisia.
[2] Department of Physics, Faculty of Applied Sciences, Umm Al-Qura University, Makkah, 21955, Saudi Arabia
[*]E-mail: othmaniabdelhak1687@gmail.com

Received: 3 March 2021 / *Accepted:* 24 April 2021 / *Published:* 30 June 2021

In this work, nanocrystalline NiO thin films of high purity are fabricated by an easy and simple sol-gel method. Several technics were used to study structural, morphological and optical properties. They proved that the particles forming the thin films are homogeneous and of an average size of 9 nm. Concerning the electrochemical properties of NiO thin films, they were studied by Cyclic Voltammetry (CV) and amperometry. CV investigations revealed that NiO nanoparticles are highly sensitive to hydrogen peroxide at an over potential of 0.05 V (vs Ag/AgCl), and amperometry measurements showed that the proposed sensor exhibits an exceptional sensitivity of 1120 $\mu A.mM^{-1}.cm^{-2}$, a fast response time (1s) and a very low detection limit of 16nM. NiO electrode proposed in this work is easy to build, inexpensive and highly stable. The excellent sensitivity, the very low detection limit and the high selectivity at very low overpotential of 0.05 V, allow the proposed sensor to be an effective candidate for H_2O_2 *in vivo* monitoring in the fields of physiology, pathology and diagnosis.

Keywords: NiO thin film**,** Non-enzymatic sensor, H_2O_2, low potential.

1. INTRODUCTION

Hydrogen peroxide (H_2O_2) is largely used in various area of industry [1-4]. In pharmaceutical, H_2O_2 is essentially used as antiseptic to prevent skin infections. As antimicrobial, it prevents the reproduction of microorganism in cosmetic products. In textile industry, it is a product of choice because it allows a high degree of brightness and conserves the mechanical properties of natural and synthetic fibres (silk, linen, cotton, wool). Likewise, hydrogen peroxide is used in environment field for soil and water treatment. H_2O_2 is also used in food industry for bleaching wheat flour, pulp, egg

white and edible oil, but the main purpose of its use is to control and to sterilize food packaging materials [5-7]. Still, their remaining residue in food can produce toxicological effects. It is therefore necessary to measure accurately H_2O_2 concentrations in common products.

Various methods are used to detect hydrogen peroxide including chemiluminescence spectrometry, chromatography, titration, and electrochemistry techniques [8, 9]. Among these techniques, the electrochemical technique is the most useful. Indeed, it is high sensitive, simple and reproducible [10, 11]. In addition, it is an inexpensive method that allows precise measurement even of nanomolar concentrations. Classic electrochemical H_2O_2 sensors are based on Horseradish Peroxidase enzyme (HRP); however, the difficult and complicated HRP immobilization as well as their high cost limits their application. To avoid these drawbacks, researches have been oriented to develop non-enzymatic sensors, ensuring the same performances or even better. During the last decades, much effort has been made to replace HRPs; noble metals and their alloys are very promising, but their use is inconvenient because of their high cost [12, 13]. For this reason, researchers oriented their attention to transition metals (Ti, Fe, Cu, Ni, Co, Mn …) and theirs oxides (TiO_2, Fe_2O_3, CuO, Cu_2O, NiO, Co_2O_3, MnO…) [14, 15]. In particular, nickel oxide (NiO) is an encouraging non-enzymatic sensor; it is abundant, non-toxic, electrochemically stable and has good catalytic activity. Similarly, NiO nanoparticles have attracted great research interest since their electron structures are differ from those of bulk materials, which can allow desirable chemical and physical properties [16, 17].

There are several techniques to manufacture NiO thin films, such as successive ionic layer adsorption (SILAR), spray pyrolysis, sol-gel, sputtering and chemical deposition [18-21]. In this work, nanocrystalline NiO thin films were carried out by sol-gel method. This method offers the advantage of developing nanomaterials of high purity and of low polydispersity. The as obtained NiO thin films were characterized by several techniques (Optical Transmission, XRD, SEM and TEM). These techniques proved that the films are formed of centered cubic (fcc) phase, having a middle size of 9 nm. Electrochemical properties of NiO thin films were studied by using cyclic voltammetry (CV) and amperometry. CV investigations revealed that NiO nanoparticles are highly sensitive to hydrogen peroxide at an over potential of 0.05 V (vs Ag/AgCl), and amperometry measurements performed at 0.05 V showed that the proposed sensor exhibits an exceptional sensitivity of 1120 $\mu A.mM^{-1}.cm^{-2}$, a fast response time (1s) and a very low detection limit of 16 nM. Similarly, the reliability of our sensor in practical applications was proven in commercial antiseptic solutions.

2. EXPERIMENTAL

2.1 Reagents and materials

Hydrogen peroxide (H_2O_2, 30%), nickel acetate tetrahydrate ($Ni(CH_3CO_2)_2.4H_2O$, 99% purity), sodium hydroxide, methanol and indium tin oxide (ITO) (R < 10 ohm/sq) were acquired from Sigma Aldrich. All chemicals are of analytical grade and used without further purification. Electrochemical experiments were performed using doubly distilled water (R = 15.8 MΩ).

2.2 Preparation of NiO thin films

The 0.3 M precursor sol was obtained by dissolving Nickel acetate tetrahydrate in methanol (99.9%) [22]. The solution was then stirred at room temperature during 3 h, until the sol became transparent and homogeneous. ITO coated glass was used as a substrate and was first Soaked under detergent at 60 °C for 10 min, rinsed and sonicated with DI water during 15 mn and then dried. The substrate was spin-coated under air atmosphere during 30 s at a speed of 2000 rpm, and then the obtained film was dried for 5 min at 100 °C. To ensure the crystallization of the coated film and the calcination of organic compounds, the sample was annealed at 500 °C during 1 h.

2.3 Measurements and apparatus

X-ray crystallographic study was made using an X'Pert³ MRD diffractometer (λ=1.5406 Å). The optical properties were studied using A Perkin Elmer Lambda 950 spectrophotometer. Concerning microscopic morphology, it was observed by scanning and transmission microscopy, using a Thermo Scientific Q250 and a Tecnai G20, respectively. The electrochemical studies were carried on a potentiostat/galvanostat AUTOLAB (PGSTAT 30) equipped with a standard three-electrode system, with the Ag/AgCl as reference electrode, platinum foil as the counter electrode and the NiO thin film as the working electrode.

3. RESULTS AND DISCUSSION

3.1. X-ray diffraction

The XRD pattern of the film annealed during 1 h at 500° C is presented in Fig. 1. Our thin films are deposited onto ITO glass; obtained peaks correspond therefore to NiO and ITO. On Fig. 1, peaks corresponding to the two materials are indexed by two different symbols.

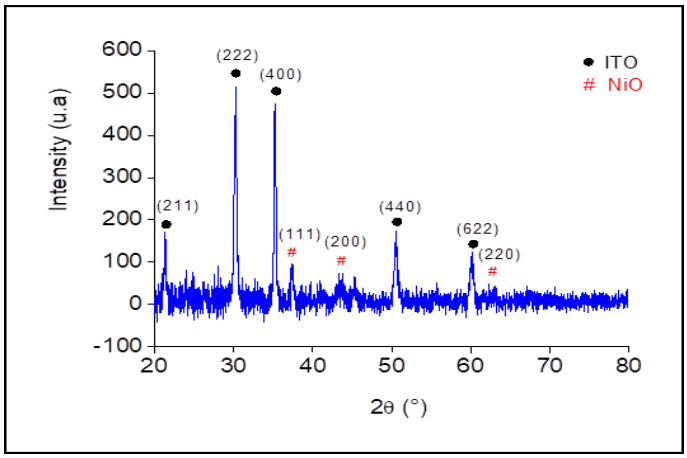

Figure 1. X-ray diffractogramme of NiO thin film coated on ITO.

The comparison with the JCPDS files allows us to differentiate these two materials, and according to the JCPDS file No.47-1049, we deduced that our thin films crystalline phase corresponds to the face-centered cubic NiO [23]. The diffraction peaks located at 37.3°, 43.3° and 62.99° correspond to (111), (200) and (220) respectively, with a lattice parameter of 4.172Å in good agreement with literature [24, 25]. There is no evidence of other NiO phase.

3.2 Electron Microscopy

The microstructure of the NiO film was examined by scanning electron microscopy (SEM) and transmission microscopy (TEM). Fig. 2a presents a cross-sectional micrograph of NiO thin film obtained by SEM. It shows that the layer is homogeneous, uniform and well adherent to the substrate surface. The thickness of the film is about 120 nm.

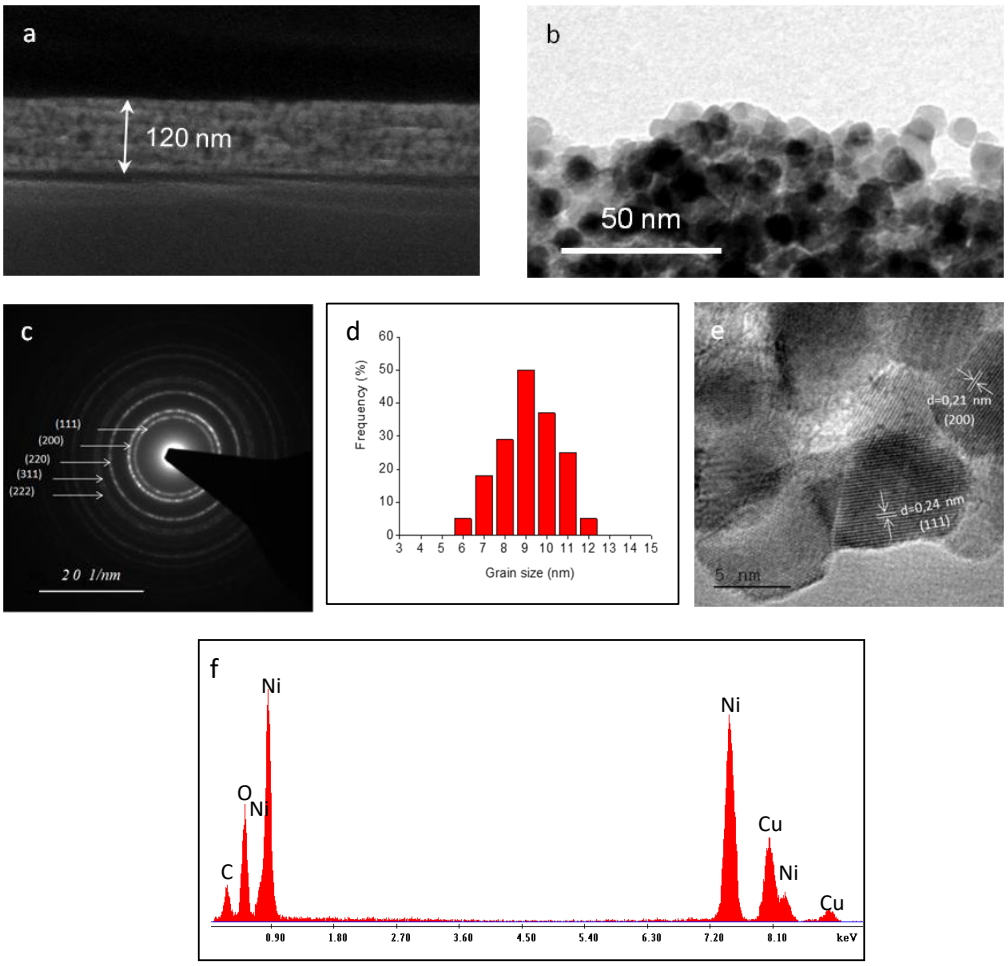

Figure 2. Microscopy analysis of NiO thin films: **a** SEM cross-section image of the NiO thin film, **b** TEM image of NiO thin film, **c** SAED pattern of NiO thin film, **d** grain size distribution histogram of NiO thin films, and **e** high-resolution transmission electron microscopy (HRTEM) image of NiO nanoparticles. **f** The EDX profile of NiO thin film confirming its high purity; carbon and copper element are due to carbon coated grid.

TEM image presented in Fig. 2b confirms that the sample is relatively dense, porous and formed by agglomerated nanoparticles. On the other hand, selected area electronic diffraction (SAED) was performed to confirm the crystalline phase of the film. The SAED pattern presented in Fig. 2c exhibits shiny distinct rings, proving the crystalline nature of the sample. The d-spacing values estimated from the SAED pattern can be perfectly attributed to face centered cubic (fcc) NiO, confirming XRD results. The nanocrystals size distribution is presented in Fig. 2d and shows a narrow distribution with an average diameter of 9 nm. The high resolution image presented in Fig. 2e confirms that NiO nanoparticles are well crystallized. In the image, two lattices spacing corresponding to (200) and (111) NiO planes are shown [26, 27]**.** The calculated lattices spacing are 0.21 and 0.24 nm, in good agreement with XRD and SAED. Energy-dispersive X-ray (EDX) was performed for elemental analysis; Fig. 2f presents the EDX spectrum of NiO film. It clearly proves that it is of high purity; carbon and copper are actually due to the carbon-coated grid.

3.3 Optical properties

In Fig. 3, we present the dependence of optical transmission of the NiO thin film covering the wavelength range of 250–1000 nm. NiO is a p type semiconductor, with a direct band-gap of 3.5 eV. We used Tauc's relation [28] to determine the optical bandgap of the elaborated NiO thin film:

$$\alpha h\upsilon = A\left(h\upsilon - E_g\right)^n \quad (1)$$

(α: absorption coefficient, $h\upsilon$: photon energy, E_g : band gap, *n=1/2* for the direct transition)

We present inset of Fig 3 the Tauc plot ($(\alpha h\upsilon)^2 = f(h\upsilon)$), where we can distinguish a linear section confirming that the band gap of NiO nanocrystals is direct. The extrapolation of the linear section gives band gap energy of 3.55 eV, in good agreement with previous works [29, 30].

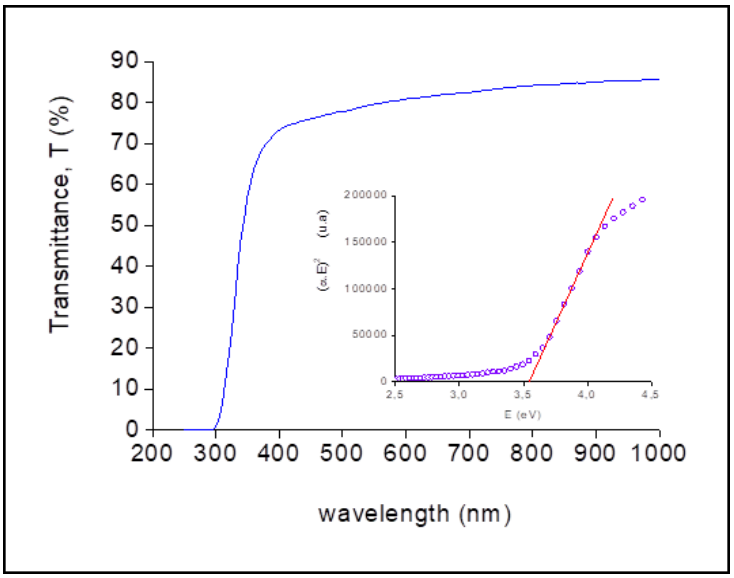

Figure 3. Optical transmission spectra of NiO thin films. Inset: Tauc law giving a band gap of 3.55 eV.

3.4 Electrochemical investigations

The electrochemical investigations of NiO thin films were achieved by voltammetry and amperometry in N_2 saturated solutions. Similarly, electrochemical analyses were performed on bare ITO as control.

3.4.1. Voltammetry investigations

We present in Fig. 4a the cyclic voltammograms (CVs) of the bare ITO and of NiO thin films, obtained at a scan rate of 50 $mV.s^{-1}$ in 0.1 M NaOH solution. The CV curve of the ITO substrate presents no obvious peak, whereas CV of the NiO thin film reveals anodic and cathodic peaks, corresponding to the oxidation/reduction of the NiO/NiOOH couple [31, 32]. In fact, when the electrode is cycled between -0.2 and 0.8 V in the alkaline solution, NiO converts first to the nickel hydroxide (Ni(II)O → Ni(III)OOH) followed by oxygen evolution reaction (OER) at potentials higher than +0.7 V. By decreasing the applied potential, reduction due to the valence transition of NiOOH to NiO occurs.

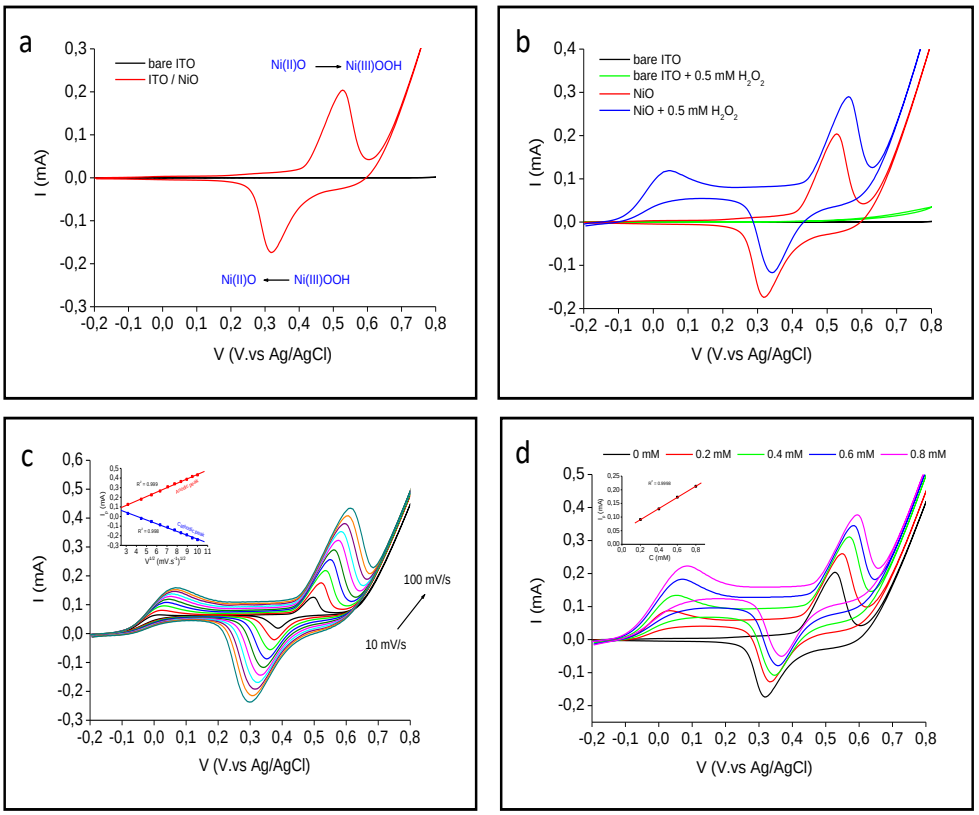

Figure 4. a CVs of NiO thin film and bare ITO performed at a scan rate of 50$mV.s^{-1}$. **b** CVs of NiO without and with 1 mM H_2O_2 at of 50$mV.s^{-1}$. **c** voltammograms of NiO film at different scan rates in presence of 1mM H_2O_2. **d** CVs recorded for different H_2O_2 concentrations, ranging from 0 to 0.8 mM; inset is The calibration curve of the electrooxidation current peak at low potentials vs H_2O_2 concentration.

The electrocatalytic oxidation of hydrogen peroxide was studied by Cyclic voltammetry in N_2 saturated 0.1 M NaOH solution. Fig. 4b exhibits CVs of NiO thin films and bare ITO performed at a scan rate of 50 mVs^{-1}, with and without 0.5 mM of hydrogen peroxide. Bare ITO presents no redox peaks, but a small enhancement of the current occurs at a potential higher than 0.4 V. Concerning the NiO film, we observe the increase of NiO oxidation peak current (I_{pa}) and the decrease of NiOOH reduction peak current (I_{pc}) which prove the excellent electrocatalytic activity of NiO thin film towards the oxidation of hydrogen peroxide by the NiO/NiOOH redox couple. This electrochemical process can be formulated as follows [33]:

$$Ni(II)O + OH^- \rightleftharpoons Ni(III)OOH + e^- \quad (2)$$

$$2Ni(III)OOH + H_2O_2 \rightleftharpoons 2Ni(II)O + 2H_2O + O_2^{\uparrow} \quad (3)$$

On the other hand, we notice that there is a non-reversible oxidation of H_2O_2 at a potential close to 0V. This H_2O_2 oxidation at low potential on the metal oxide surface has already been observed. Recently, Sivakumar et al. [34] observed an oxidation of hydrogen peroxide on the NiO surface at a potential of 0.13V. Similarly, Gao et al. [35] also observed an equivalent behaviour of hydrogen peroxide on the surface of $Ni(OH)_2$ modified electrodes.

Figure 4c corresponds to cyclic voltammetry plots recorded at different scan rates in the presence of 0.5 mM of hydrogen peroxide. It is observed that the current density of oxidation (I_{pa}) and reduction (I_{pc}) peaks is proportional to the square root of the scan rates, indicating that the electrooxidation of hydrogen peroxide correspond to a diffusion-controlled process. Fig. 4d displays CVs responses for different hydrogen peroxide concentrations ranging from 0 to 0.8 mM. The calibration curve inset shows that the electrooxidation current peak at low potentials is linear to hydrogen peroxide concentration. H_2O_2 sensors based on the redox reactions of metal oxides are disturbed by interfering species, but a sensor operating at 0.05 V could avoid common anodic and cathodic interferences induced by interfering substances such as glucose, uric acid and ascorbic acid. Consequently, our choice was to study by amperometry, the performances of the proposed sensor at an applied potential of 0.05 V.

3.4.2 Amperometric studies

The sensing merits of our NiO thin films at the applied potentials of 0.05 V were studied by amperometric method, using three electrodes cell. The 0.1 M NaOH solution was N_2 saturated and stirred at 300 rpm.

Fig. 4a shows the response of NiO film to successive H_2O_2 additions at an applied potential of 0.05 V ranging from 0.0005 to 10 mM. As it can be seen, the oxidation current increases steeply with increasing hydrogen peroxide concentration and it attain a steady-state level within only 1s, demonstrating a rapid and sensitive response to the analyte. We also observe that the current is stable even for high-added concentrations (10 mM) which proves that our film is well adherent and is not deteriorated by hydrogen peroxide addition. The corresponding calibration curve for H_2O_2 concentrations ranging from 0.00005 to 3mM is presented in Fig. 4b. The sensitivity deduced with good correlation coefficients (R^2> 0.99), is 1120 $\mu A.mM^{-1}.cm^{-}1$, which is exceptionally high. To our

best knowledge, it is among if not the highest for H_2O_2 sensing at an applied potential of 0.05 V, found in literature. Likewise, the proposed sensor displays a fast response of 1s and a linear range from 0.0005 to 0.6 mM.

Fig. 4c presents the amperogram of the lowest added concentrations (50, 100, 150, and 200 nM), and as it can be seen, the calibration of oxidation current displayed in Fig. 4d, is rigorously linear to the H_2O_2 concentration (R^2 = 0.9999). According to the IUPAC definition [36], a signal can be considered as a true signal when it is superior to 3 times the standard deviation of noise (S/N = 3). Thus, the limit of detection (LOD) can be deduced from the linear calibration curve when the signal equals 3 times the noise.

$$LOD = \frac{3rmsd}{sensitivity} \qquad (4)$$

Using the above Eq. (6), the LOD was deduced to be 16 nM.

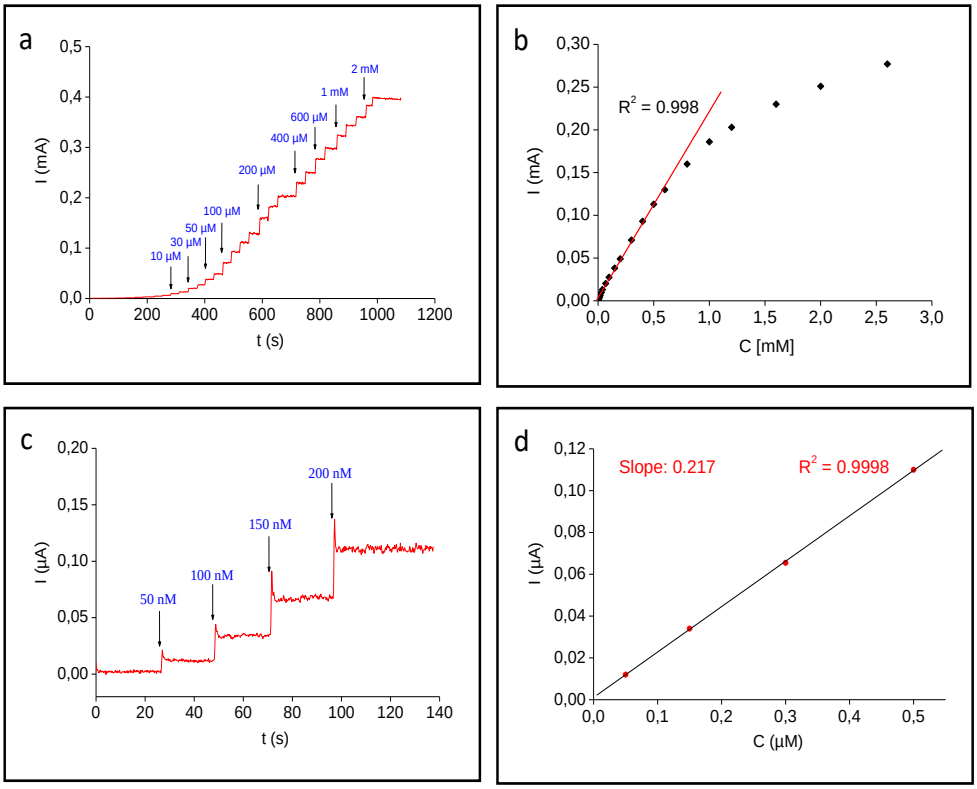

Figure 5. a Amperometric response to successive H_2O_2 additions performed at 0.05 V vs Ag/AgCl, and **b** its corresponding calibration curve. **c** The response to 50, 100, 150 and 200 nM of H_2O_2 successive additions, and **d** the corresponding plot of I=f (C)

In table 1, we summarize the sensing performances of typical low potentials electrochemical H_2O_2 sensors based on precious metal and metal oxides. The comparison reveals that NiO thin films presented in this work display the highest sensitivity at 0.05 V. Furthermore, it exhibits appreciable performances in terms of detection limit and linear range. The hydrogen peroxide sensors at low potential (-0.2 → +0.2V) proposed in literature, are mostly based on noble metals and their alloys [38-

46], nevertheless their cost and the often complicated preparation method limits their use. Some metal oxides are recently proposed as hydrogen peroxide sensors at low potentials [34-35, 37]. It is noted that even though the modified electrodes of NiO and $Ni(OH)_2$ are sensitive to H_2O_2 at low potential, the sensitivity of our electrode is far better. Similarly, the electrode prepared by Gao et al. exhibits extremely low limit detection, however, its use may be limited by the use of the rotating electrode. We believe that the excellent performance of our electrode can be attributed to the quality of the film. Indeed, the NiO nanoparticles presented in this work are of high purity, very small size with a narrow distribution. Therefore, these nanoparticles have a substantial fraction of their atoms on the surface, implying an increase of under-coordinated atoms; we think that they possess the ability to catalyze H_2O_2 at 0.05 V.

Table 1. Comparison of the performances of typical low potentials non-enzymatic and precious metal electrochemical H_2O_2 sensors.

Sensors	Applied Potential (V.vs Ag/AgCl)	Sensitivity ($\mu A.mM^{-1}.cm^{-2}$)	Linear range (mM)	Detection limit (µM)	Ref.
GDC/NiO-modified GCE	+0.13	107.22	0.01-3.9	0.0015	[34]
Ni(OH)2/ERGOMWNT/GCE	+0.2	717	0.1-9.05	4	[35]
CQDs/octahedral Cu_2O	-0.2	130	0.005-5.3	2.8	[37]
Silver nanowire	-0.2	0.0266	0.1-3.1	29.2	[38]
GO/AuNPs/CS	-0.2	99.5	0.2-4.2	-	[39]
PDDA/t-GO-Pt/GCE	-0.1	-	0.001-5	0.65	[40]
RGO/CNTs-Pt/GCE	-0.2	347	0.1-4	1.2	[41]
GN-Pt/GCE	0	-	0.002-0.71	0.5	[42]
MWCNTs-Pt NPs/Pt	0	205.8	0. 01-2	0.3	[43]
Nafion/PtNPs/RGO	0	39.89	0.01-15	3.1	[44]
PVA-MWCNTs-Pt NPs	0	122.63	0.002-3.8	0.7	[45]
rGO-PANI-Pt NP/GCE	0	257.04	0.02-8	1.1	[46]
NiO thin films	0.05	1120	0-0.6	0.016	**This work**

GO: graphene oxide, CS: chitosan, PDDA: polydiallydimethylammonium, GCE: glassy carbon electrode, GN: graphene, MWCNTs: multiwalled carbon nanotubes, PVA: polyvinylalcohol, rGO: reduced graphene oxide, PANI: polyaniline, CQDs: carbon quantum dots, ERGOMWNT: electroreduced graphene oxide multiwalled carbon nanotube, GDC: glucose derivedsheet-likecarbons.

3.4.3. Interference, stability and reproducibility studies

The discrimination of interference species is one of the most important challenges of non-enzymatic sensors. Indeed, real samples may contain substances such uric acid (UA), ascorbic acid (AA) and glucose, which are able to affect H_2O_2 detection. It is therefore necessary to study their impact; the interference test was evaluated by amperometry in an N_2 saturated 0.1 M NaOH solution at the over potential of 0.05 V. In first step, we added 0.1 mM of H_2O_2 and the interference of ascorbic acid, uric acid and urea were studied by injecting 0.01 mM of the respective solutions. The second adding of 0.1 M of H_2O_2 is followed by the successive adding of 0.1mM of glucose, glycine, $NaNO_3$,

KNO_3, NaCl and KOH. It is noted that the injection of H_2O_2 causes a significant and sudden increase of the current signal, this increase is on the other hand much lower after the addition of ascorbic and uric acids. The small interference due to AA and UA are the oxidation of these substances on the surface of NiO electrode [47]. The adding of all other interfering species does not affect the signal. The fact that there is no response to glucose adding at 0.05 V challenged us, therefore, the response of our sensor to glucose was investigated by cyclic voltammetry measurements in N_2 saturated 0.1 M NaOH solution. The result is presented in Fig. 6b, where we observe that the addition of 1 mM of glucose has no effect at the potentials ranging from 0 to 0.3 V, confirming the result observed by interference study. Within the biological environments, glucose, AA and UA are usually co-existent with H_2O_2, and thanks to its high selectivity against these species at 0.05 V, the proposed sensors can be appropriate to *in-vivo* experiments.

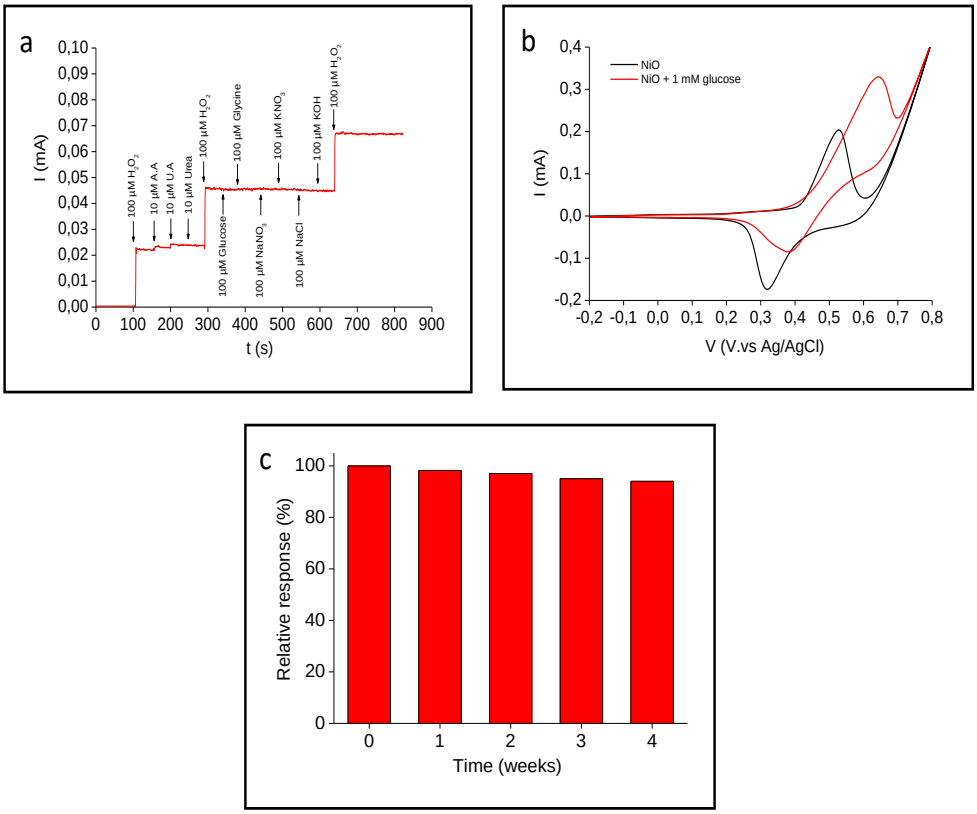

Figure 6. **a** Interferences response of NiO thin films at an applied potential of 0.05 V. **b** Cyclic Voltammograms of NiO thin film with and without 1 mM Glucose at rate scan of 50mV.s^{-1} in 0.1M NaOH. **c** Long-term stability of NiO thin films response towards 0.2 mM H_2O_2 during four successive weeks at an applied potentials of 0.05 V.

Reproducibility and stability are two important parameters for checking sensors efficiency. The reproducibility and the storage stability of NiO thin films where tested by amperometric measurements in 0.1 M NaOH. To assess the reproducibility, five different NiO thin films prepared by sol-gel method, were tested individually with 0.2 mM of H_2O_2. The relative standard deviation (RSD) was determined to be 2.7 %, which proves the good reproducibility of the proposed sensor. Furthermore,

the stability was investigated by measuring the current response at the over potential of 0.05 V, to 0.2 mM H_2O_2 each week during 1 month. The sample was stored at room temperature and as seen in Figure 6c, it preserves 98% of its initial response. Thus, NiO electrode fabricated by sol-gel has the potential to be used as H_2O_2 sensors with high reproducibility and stability.

3.4.4 Real sample analysis

The practicability of the developed sensor was proved by testing two local commercial disinfectants (H_2O_2 solution of 3%). The test was by using a standard addition method in 0.1 M NaOH at the applied potential of 0.05 V. The NiO thin film electrode presents acceptable recoveries, as shown in table 3. Accordingly, the proposed electrode can be effectively used for H_2O_2 determination in a real-time application.

Table 2. H_2O_2 detection in commercial disinfectant solutions by NiO thin film.

Sample	Applied potential (V)	H_2O_2 added (µM)	H_2O_2 found (µM)	RSD (n = 5)	Recovery (%)
A	0.05	100	98	2.9	98 %
B	0.05	100	99	2.7	99 %

4. CONCLUSION

High purity NiO thin films were deposited on ITO substrate by a facile sol-gel method. Structural and morphological characterizations showed that the obtained NiO thin films are formed by face-centered structure nanoparticles, having an average size of 9 nm. CV investigations revealed that NiO nanoparticles are highly sensitive to hydrogen peroxide at low potentials (around 0 V vs Ag/AgCl). In the same way, amperometric measurements performed at 0.05 V showed excellent sensing performances toward H_2O_2 detection. The sensitivity of the proposed sensor at a very low overpotential is among the highest found in literature. Additionally, it displays a fast response time, a very low detection limit and a wide linear. Additionally, NiO thin films of the present work are highly selective, stable and reproducible. The excellent anti-interference properties allowed the accurate determination of H_2O_2 in commercial antiseptic solutions, with an excellent recovery. More, the very low detection limit and the high selectivity at an applied potential of 0.05 V, allow the proposed sensor to be an effective candidate for H_2O_2 sensing in biologic fields, physiology, pathology and diagnosis.

DECLARATION OF INTEREST

The authors declare that they have no known competing financial interests or personal relationships that could have appeared to influence the work reported in this paper.

DATA AVAILABILITY STATEMENT

The data that support the findings of this study are available from the corresponding author.

References

1. E. Aziz, M. Fazlzadeh, M. Ghayebzadeh, L. Hemati, M. Beikmohammadi, H.R. Ghaffari, H. R. Zakeri and K. Sharafi, *Environ. Protection Eng.*, 43 (2017) 183.
2. C. Kilicarislan-Ozkan, H. Ozgunay, H, Akat, *Int. J. Biol. Macromol.*, 122 (2019) 610.
3. L.C. Neves, J.B. de Souza, C.M. de Souza Vidal, L.T. Herbert, K.V. de Souza, K.G. Martins, B.J. Young, *Ecotoxicol. Environ. Saf.*, 202 (2020) 110939.
4. J.W. Lee, J.D. Helmann, *Nature*, 440 (2006) 363.
5. W. Chen, S. Cai, Q.Q. Ren, W. Wen, Y.D. Zhao, *Analyst*, 137 (2012) 49.
6. M. Swieca, *Food Chem*., 180 (2015) 219.
7. N. Scaramuzza, M. Cigarini, P. Mutti, E. Berni, *Int. J. Food Microbiol.*, 316 (2020) 108421
8. M. Song, J. Wang, B. Chen, L. Wang, *Anal. Chem.*, 89 (2017) 11537.
9. P.P. Waifalkar, A.D. Chougale, P. Kollu, P.S. Patil, P.B. Patil, *Colloids Surf. B*, 167 (2018) 425.
10. K. Zhan, H. Liu, H. Zhang, Y. Chen, H. Ni, M. Wu, D. Sun, Y. Chen, *J. Electroanal. Chem.,* 724 (2014) 80.
11. C. Xu, L. Zhang, L. Liu, Y. Shi, H. Wang, X. Wang, F. Wang, B. Yuan, D. Zhang, *J. Electroanal. Chem.,* 731 (2014) 67.
12. N.Wang, Y.Han, Y.Xu, C.Gao, X.Cao, *Anal. Chem*. 87 (2015) 457.
13. H. Li, W.Hao, J. Hu, H. Wu, *Biosens. Bioelectron*., 47 (2013) 225.
14. F.J. Garcia-Garcia, P. Salazar, F. Yubero, A.R. González-Elipe, *Electrochim. Acta*, 201 (2016) 38.
15. G. Zeng, W. Li, S. Ci, J. Jia, Z.Wen, *Sci. Rep*., 6 (2016) 36454.
16. M. Guziewicz, P. Klata, J.Grochowski, K. Golaszewska, E. Kaminska, J.Z. Domagala, B.A. Witkowski, M. Kandyla, C. Chatzimanolis, M. Kompitsas, A. Piotrowska, *Procedia Eng*., 47 (2012) 746.
17. Z. Ibupoto, K. Khun, V. Beni, M. Willander, *Soft Nanosci. Lett*., 3 (2013) 46.
18. A.M. Reddy, A.S. Reddy, K.S. Lee, P.S. Reddy, *Solid State Sci*., 13 (2011) 314.
19. R. Swartwout, M. T. Hoerantner, V. Bulović, *Energy Environ. Mater.*, 2 (2019) 119.
20. S. Naghdi, K. Rhee, D. Hui, S. Park, *Coatings,* 8 (2018) 278.
21. X.H. Chan, J. R. Jennings, M.A. Hossain, K.K.Z. Yu, Q. Wang, *J. Electrochem. Soc*., 158 (2011) 733.
22. N. Talebian, M. Kheiri, *Solid State Sci*. 27 (2014) 79.
23. K. Nguyen, N.D. Hoa, C.M. Hung, D.D.T. Le, N.V. Duy, N.V. Hieu, *RSC Adv*., 8 (2018) 19449.
24. M. El-Kemary, N. Nagy, I. El-Mehasseb, *Mater. Sci. Semicond. Process.,* 16 (2013) 1747.
25. E.R. Shaaban, M.A. Kaid, M.G.S. Ali, *J. Alloy. Compd*., 613 (2014) 324.
26. S. Rakshit, S. Ghosh, S. Chall, S.S. Mati, S.P. Moulik, S.C. Bhattacharya, *RSC Adv*., 3 (2013) 19348.
27. F.E. Atalay, D. Asma, H. Kaya, A. Bingol, P. Yaya, *Nanomater. Nanotechnol.,* 6 (2016) 28
28. J.B. Coulter, D.P. Birnie, *Phys. Status Solidi B Basic Res.*, 255 (2018) 1700393.
29. B. Saha, K. Sarkar, A. Bera, K. Deb, R. Thapa, *Appl. Surf. Sci*., 418 (2017) 328.
30. H.K. Li, T.P. Chen, S.G. Hu, X.D. Li, Y. Liu, P.S. Lee, X.P. Wang, H.Y. Li, G.Q. Lo, *Opt. Express*., 23 (2015) 27683.
31. Y. Ren, X. Zhou, H. Zhang, L. Lei, G. Zhao, *J. Mater. Chem. C,* 6 (2018) 4952.

32. A. Amirzhanova, I. Karakaya, C.B. Uzundal, G. Karaoğlu, F. Karadas, B. Ülgüt, Ö. Dag, *J. Mater. Chem. A*, 7 (2019) 22012.
33. W. Liu, H. Zhang, B. Yang, Z. Li, L. Lei, X. Zhang, *J. Electroanal. Chem*., 749 (2015) 62.
34. M. Sivakumar, V.Veeramani, S.M. Chen, R.Madhu, S.B. Liu, *Microchim. Acta*, 186 (2019) 59
35. W. Gao, W.W. Tjiu, J. Wei, T. Liu, *Talanta,* 120 (2014) 484.
36. L.A. Currie, *Pure Appl. Chem.*, 67 (1995) 1699.
37. Y.C. Li, Y.M. Zhong, Y.Y. Zhang, W. Weng, S.X. Li, *Sens. Actuators B chem*., 206 (2015) 735.
38. E. Kurowska, A. Brzozka, M. Jarosz, G.D. Sulka, M. Jaskula, *Electrochim. Acta***,** 104 (2013) 439.
39. K. Yang , H. Zhong, Z.P. Cheng, X.R. Li , A.R. Zhang, T.L. Li , Y.J. Zhang , G.Q. Liu, H.Y Qian, *J. Electroanal. Chem.*, 814 (2018) 1.
40. J.M. You, D. Kim, S. Jeon, *Electrochim. Acta*, 65 (2012) 288.
41. Y. Zhang, Q. Cao, F. Zhu, H. Xu, Y. Zhang, W. Xu, X. Liao, *Int. J. Electrochem. Sci.*, 15 (2020) 8771.
42. F. Xu, Y. Sun, Y. Zhang, Y. Shi, Z. Wen, Z. Li, *Electrochem. Commun*., 13 (2011) 1131.
43. Z. Miao, D. Zhang, Q. Chen, *Materials,* 7 (2014) 2945.
44. H. Qi, J. Song, Y. Fu, X. Wu, H. *Nanotechnology*, 31 (2020) 135503.
45. Y. Fang, D. Zhang, X. Qin, Z. Miao, S. Takahashi, J.I. Anzai, Q. Chen, *Electrochim. Acta,* 70 (2012) 266.
46. X. Du, Y. Chen, W. Dong, B. Han, M. Liu, Q. Chen, J. Zhou, *Oncotarget*, 8 (2017) 13039.
47. S. Wang, C. Wang, G. Wei, H. Xiao, N. An, Y, Zhou, C, An, J. Zhang, *Colloids Surf. A Physicochem. Eng. Asp*., 509 (2016) 252.